

Electronic Spectroscopy and Photodissociation Dynamics of Hydrated Co^{2+} Clusters: $\text{Co}^{2+}(\text{H}_2\text{O})_n$ ($n = 4-7$)

Kieron P. Faherty, Christopher J. Thompson, Fernando Aguirre, Jodi Michne, and Ricardo B. Metz*

Department of Chemistry, University of Massachusetts, Amherst, Massachusetts 01003

Received: April 18, 2001; In Final Form: August 20, 2001

Solvated cluster ions $\text{Co}^{2+}(\text{H}_2\text{O})_n$ with $n = 4-7$ have been generated by electrospray ionization and studied by laser photofragment spectroscopy. The similarity between the spectrum of gas-phase $\text{Co}^{2+}(\text{H}_2\text{O})_6$ and the absorption spectrum of aqueous cobalt(II) suggests that $\text{Co}^{2+}(\text{H}_2\text{O})_{6(\text{aq})}$ is responsible for the room-temperature solution absorption spectrum. The observed photodissociation spectrum of $\text{Co}^{2+}(\text{H}_2\text{O})_4$ is similar to new bands which appear in aqueous cobalt(II) at high temperatures and have been assigned to $\text{Co}^{2+}(\text{H}_2\text{O})_{4(\text{aq})}$ by Swaddle and Fabes (Swaddle, T. W.; Fabes, L. *Can. J. Chem.* **1980**, *58*, 1418–1426). The hexahydrate was found to dissociate by loss of one or two water molecules, whereas the heptahydrate dissociates by loss of two or three water molecules. In both cases, loss of two water molecules is the preferred dissociation pathway. The tetrahydrate dissociates either by simple loss of water or by charge separation to form $\text{CoOH}^+(\text{H}_2\text{O})_2$ and H_3O^+ , with charge separation being the preferred dissociation channel. At 570 nm, photodissociation by charge separation leads to a kinetic energy release of 110 ± 20 kJ/mol, 48% of the available energy. This modest kinetic energy release is consistent with a “salt bridge” mechanism.

Introduction

In aqueous solution, first-row transition metal dications (M^{2+}) are surrounded by an inner solvation shell of six water molecules, resulting in an octahedral or near-octahedral species.¹ Crystal field theory states that the resulting field splits the degenerate atomic 3d orbitals into molecular e_g and t_{2g} orbitals. The traditional view is that the characteristic absorption bands in the visible and near-ultraviolet regions are due to transitions between these molecular orbitals.^{2,3} The observed transitions are quite weak, with typical² extinction coefficients $\epsilon \approx 1-10$ $\text{M}^{-1} \text{cm}^{-1}$. As d–d transitions are symmetry forbidden in isolated M^{2+} and for M^{2+} in a potential containing a center of inversion (e.g., octahedral), the observation of these symmetry-forbidden transitions is usually attributed to vibronic coupling in the complex.^{2,4}

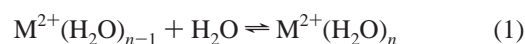
In a recent paper,⁵ Gilson and Krauss challenge the traditional interpretation of the d–d absorption spectra of transition metal ions. They studied $\text{Co}^{2+}(\text{H}_2\text{O})_n$ ($n = 4-6$), computing energies and intensities for transitions to the 10 lowest-lying electronic states using complete active space multiconfigurational self-consistent field theory (CAS-MCSCF) and multiconfigurational quasi-degenerate perturbation theory (MCQDPT). They propose that although $\text{Co}^{2+}(\text{H}_2\text{O})_6$ is the major species in solution, it is not responsible for the visible aqueous absorption due to the low oscillator strength ($f < 10^{-6}$) for its electronic transitions in the visible. They concluded that the observed spectra are caused by a mixture of thermodynamically disfavored but relatively strongly absorbing species, with the largest contribution coming from $\text{Co}^{2+}(\text{H}_2\text{O})_5$. The pentahydrate is an important intermediate of water exchange by aqueous Co^{2+} .⁶⁻⁸ They also suggest that $\text{Co}^{2+}(\text{H}_2\text{O})_4$ may contribute to the spectrum, especially at high temperatures.

Swaddle and Fabes⁹ measured the absorption spectra of Co(II) solution at five temperatures from 290 to 625 K. Significantly above room temperature, they observe two new bands in the absorption spectrum at 552 and 486 nm whose intensity increases rapidly with temperature. These high-temperature features were assigned to $\text{Co}^{2+}(\text{H}_2\text{O})_{4(\text{aq})}$. Recently, Swaddle reasserted that high-pressure experiments suggest that $\text{Co}^{2+}(\text{H}_2\text{O})_6$ rather than $\text{Co}^{2+}(\text{H}_2\text{O})_5$ is responsible for the room temperature solution spectrum based on their experiments and data previously obtained by other techniques.¹⁰ This interpretation has been contested by Gilson and Krauss.¹¹

Gas phase molecular clusters have been extensively investigated in order to understand the evolution of properties such as ion solvation, structure, and dynamics from isolated gas-phase molecules to the condensed phase.^{12,13} Measuring the absorption of size selected clusters allows us to identify the carrier of the solution spectrum and to obtain the spectra of coordinatively unsaturated ions that are difficult to produce in the condensed phase.

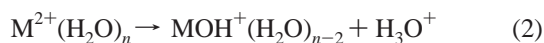
Although a great deal of work has been carried out on clusters of alkali and alkaline earth metal ions with water,^{12,13} multiply charged transition metal clusters have been less extensively studied due to the historical difficulty of producing them in the gas phase. The introduction of electrospray ionization mass spectrometry (ESI-MS) by Yamashita and Fenn¹⁴ in the mid-1980s has allowed increased access to multiply charged metal-containing species.

Several research groups have examined the transition metal $\text{M}^{2+}(\text{H}_2\text{O})_n$ systems using mass spectrometric techniques. The only previous study of cobalt-containing clusters is by Kebarle and co-workers who determined ΔG° values of hydration by measuring the equilibrium for the hydration reaction



* To whom all correspondence should be addressed. E-mail: rbmetz@chemistry.umass.edu.

for transition metals from Mn to Zn.^{15,16} These studies were limited to $n = 8-13$ due to the design of their apparatus. By assuming the entropy $\Delta S^\circ = 96$ J/K mol they obtained average outer-solvation shell hydration energies of ~ 63 kJ/mol.^{15,16} Collision-induced dissociation (CID) studies showed that loss of water is the major channel for dissociation and increases in importance with increasing n . A charge reduction channel was also observed for clusters containing fewer than a critical number of water ligands



The critical number of water ligands required for charge reduction depends on the second ionization energy of the metal and the nature of the ligand. From CID studies, they were able to estimate that the first three water molecules are bound to Co²⁺ by an *average* of ~ 250 kJ/mol each.¹⁵

Photofragment spectroscopy has been extensively used to study singly charged ions and has recently been applied to the study of transition metal-containing dications. Posey and co-workers^{17,18} have used photofragment spectroscopy to study Fe²⁺(bpy)₃, Fe²⁺(terpy)₂, and other ligated transition metal dications solvated by molecules such as methanol and DMSO. They studied the effect of the nature and number of solvent molecules on the strongly allowed metal-to-ligand charge-transfer band. The photodissociation spectra obtained are similar to the solution spectra but shifted to shorter wavelength as the number of methanol solvent molecules decreases. This implies that the oxidation number of the metal in solution is retained in the gas phase.¹⁷

Recently, our group has carried out work on Ni²⁺(H₂O)_{*n*} complexes, focusing on $n = 4-7$.¹⁹ Using photofragment spectroscopy in the region 720–840 nm, it was found that the hexa- and heptahydrates photodissociate via simple loss of a water molecule. The tetrahydrate dissociates exclusively via charge reduction. Photodissociation of the pentahydrate was not observed.

There have been few theoretical studies of hydrated transition metal dications. Åkesson et al. used MCSCF methods to find the total binding energy of six H₂O molecules to a first-row transition metal center, giving an *average* bond strength of 200 kJ/mol.²⁰ This accounts for 75% of the total solvation energy of M²⁺. Pavlov and co-workers used the B3LYP method to find *sequential* binding energies of the first six water molecules to Zn²⁺.²¹ Their results show that the sequential solvation energies decrease with increasing n , with the sixth water bound by 91 kJ/mol and the fifth by 100 kJ/mol. Because binding energies are primarily electrostatic in nature and the calculated²⁰ total binding energies of six H₂O to Co²⁺ and Zn²⁺ differ by only 3%, the sequential bond energies in Co²⁺(H₂O)_{*n*} should be similar to those calculated for Zn²⁺(H₂O)_{*n*}.

In this work, we investigate the absorption properties of gas-phase Co²⁺(H₂O)_{*n*} ($n = 4-7$) cluster ions. Also, dissociation channels and kinetic energy release are monitored as a function of the number of water ligands. This is part of a series of studies of the solvation of the first-row transition metal ions, M²⁺, which commenced with the study of Ni²⁺.¹⁹

Experimental Section

Gas-phase Co²⁺(H₂O)_{*n*} clusters are studied using a reflectron time-of-flight photofragment spectrometer.²² In the custom electrospray source,¹⁹ cluster ions are formed under atmospheric pressure by flowing a 5.0×10^{-4} M solution of CoCl₂ in distilled water at a rate of 0.75 mL/h through a stainless steel

needle held at 6.75 kV. The ions enter a differentially pumped chamber maintained at ~ 1 Torr through a heated 18.4 cm long, 0.51 mm i.d., 1.59 mm o.d. stainless steel desolvation tube held between 0 and 100 V, then pass through a skimmer into a second differentially pumped chamber held at 4.5×10^{-4} Torr. The potential difference between the desolvation tube and skimmer is varied from 0 to 10 V to optimize the ion signal. An octopole then guides ions into an rf ion trap. This trap enables the continuous electrospray source to be coupled to the inherently pulsed time-of-flight mass spectrometer.^{23,24} Ions are acquired in the ion trap for up to 49 ms, during which time they are thermalized to 300 K by collisions with helium bath gas and residual air.¹⁹ Upon ejection from the trap, the ions are accelerated through a potential of 1800 V and are re-referenced to ground potential.²⁵ An Einzel lens and a series of deflector plates guide the ion packet through a field-free region and into the reflectron. At the turning point of the reflectron the mass-selected clusters are excited using the unfocused output of a dye laser pumped by the second or third harmonic of a Nd:YAG laser operating at 20 Hz repetition rate. The fragments pass through a second field-free region to a microchannel plate detector. Photodissociation pathways are determined from *difference spectra* – the difference between time-of-flight spectra obtained with the laser blocked and unblocked. Photodissociation cross sections are determined by integrating the area under the fragment peaks in the difference spectrum, dividing by the area of the parent ion peak in the time-of-flight spectrum and by the laser fluence. Uncertainties in the absolute cross sections are estimated at 50% and are due to laser beam nonuniformity and uncertainty in the overlap between the laser and ion beams.¹⁹ Careful power dependence studies show that the branching between fragment channels is independent of laser power and fragment ion yield is linear with laser fluence over the range measured ($< 0.1-0.6$ J/cm²), indicating that the effect of multiphoton processes is minimal. To minimize saturation effects the laser is attenuated, where necessary, to maintain total photodissociation below 15%. Because the clusters studied have very small photodissociation cross sections, *photodissociation spectra* are obtained by measuring the photodissociation cross section as described above as a function of photolysis wavelength.

Results and Discussion

Several cluster ions Co²⁺(H₂O)_{*n*} have been observed, and clusters with $n = 4-7$ are examined in the range 460–660 nm. Only small amounts of the pentahydrate could be generated and no photodissociation was observed. This is consistent with our results for Ni²⁺(H₂O)₅, where photodissociation of the pentahydrate was immeasurably small.¹⁹

The photodissociation spectrum of a molecule mirrors its absorption spectrum if absorption of light always leads to photodissociation. Williams and co-workers determined the binding energy of the sixth water molecule in Ni²⁺(H₂O)₆ to be 8400 cm⁻¹ using the blackbody infrared radiation technique.²⁶ We expect water to be bound in Co²⁺(H₂O)₆ by a similar amount based on the calculations of Åkesson et al.²⁰ As a 660 nm photon provides 15 150 cm⁻¹ of energy, well above the expected binding energy of the sixth water molecule, absorption should lead to fragmentation.

Aqueous Co²⁺ has two absorption peaks in the visible and near-ultraviolet: a peak at 515 nm ($\epsilon \approx 4.6$ M⁻¹ cm⁻¹) and a small shoulder at 465 nm ($\epsilon \approx 2.6$ M⁻¹ cm⁻¹). Traditionally, these transitions have been assigned to symmetry forbidden

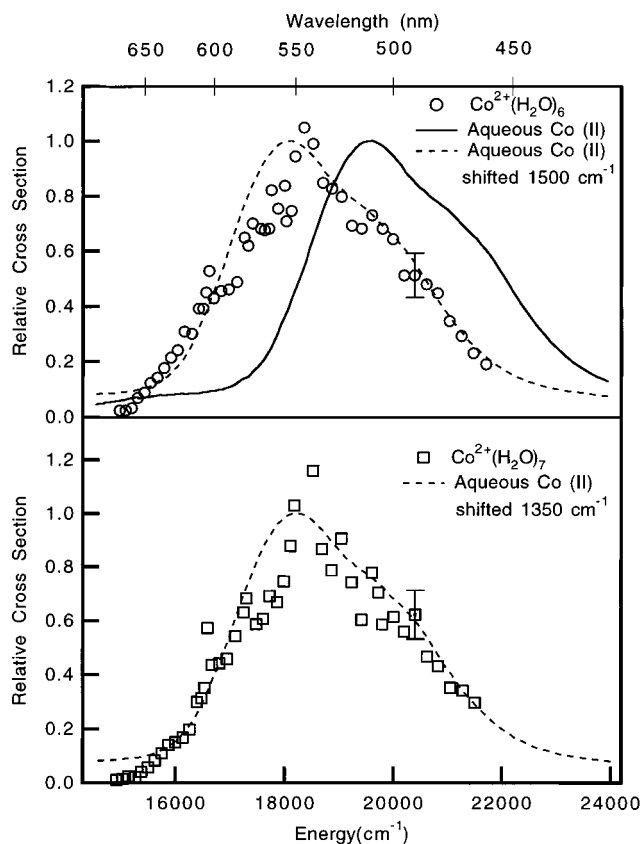


Figure 1. Top, Comparison of total photodissociation spectrum of $\text{Co}^{2+}(\text{H}_2\text{O})_6$ (circles) to the absorption spectrum of aqueous cobalt(II) chloride and to the aqueous absorption spectrum shifted 1500 cm^{-1} to lower energy. A relative cross section of one corresponds to $\epsilon = 6 \times 10^{-20}\text{ cm}^2$ for $\text{Co}^{2+}(\text{H}_2\text{O})_6$ and $\epsilon = 4.6\text{ M}^{-1}\text{ cm}^{-1}$ for aqueous CoCl_2 . Bottom, Total photodissociation spectrum of $\text{Co}^{2+}(\text{H}_2\text{O})_7$ (squares). A relative cross section of one corresponds to $\sigma = 5 \times 10^{-20}\text{ cm}^2$ for $\text{Co}^{2+}(\text{H}_2\text{O})_7$. Also shown for comparison is the absorption spectrum of aqueous cobalt(II) chloride, shifted 1350 cm^{-1} to lower energy.

d-d transitions in the octahedral $\text{Co}^{2+}(\text{H}_2\text{O})_6$ species, with the explanation that the transitions are weakly vibronically allowed.^{2,4}

Larger Clusters: $\text{Co}^{2+}(\text{H}_2\text{O})_n$ ($n = 6, 7$). Figure 1 (top) compares the total photodissociation spectrum of $\text{Co}^{2+}(\text{H}_2\text{O})_6$ to the aqueous absorption spectrum of cobalt(II). The observed spectrum is very similar in appearance to that of the solution, but is shifted to lower energies by approximately 1500 cm^{-1} , with the peak occurring at 18350 cm^{-1} . The maximum photodissociation cross section of the cluster is $\sigma = 6 \times 10^{-20}\text{ cm}^2$, which corresponds to an extinction coefficient of $\epsilon \approx 37\text{ M}^{-1}\text{ cm}^{-1}$. The $\text{Co}^{2+}(\text{H}_2\text{O})_6$ cross section is larger than the $2 \times 10^{-20}\text{ cm}^2$ measured for $\text{Ni}^{2+}(\text{H}_2\text{O})_6$ previously.¹⁹ The error bars shown in the figure represent uncertainties in relative cross section; as noted above, uncertainties in the absolute cross sections are estimated at 50%.

According to the calculations of Gilson and Krauss,⁵ in octahedral $\text{Co}(\text{H}_2\text{O})_6^{2+}$ the $4\text{F}(3\text{d}^7)$ ground state of isolated Co^{2+} is split into the ground $4\text{T}_{1\text{g}}$ state, a $4\text{T}_{2\text{g}}$ state at $\sim 6700\text{ cm}^{-1}$ and a 4A_2 state near 14000 cm^{-1} . The $4\text{T}_{1\text{g}}(\text{P})$ state near 20500 cm^{-1} arises from the $4\text{P}(3\text{d}^7)$ excited state of Co^{2+} . Calculations^{5,27} and a wide body of work^{2,3} on octahedral Co^{2+} complexes with oxygen-containing ligands thus suggest that the $4\text{T}_{1\text{g}}(\text{P}) \leftarrow 4\text{T}_{1\text{g}}$ transition is responsible for the visible absorption spectrum of $\text{Co}(\text{H}_2\text{O})_6^{2+}$. Allowing the cluster geometry to fully relax (which slightly distorts the symmetry from octahedral) and including spin-orbit interactions splits the $4\text{T}_{1\text{g}}$ ground state

into six states spanning 1100 cm^{-1} and the $4\text{T}_{1\text{g}}(\text{P})$ excited state into six states spanning 1200 cm^{-1} . The calculated $4\text{T}_{1\text{g}}(\text{P}) \leftarrow 4\text{T}_{1\text{g}}$ transition energy of 20500 cm^{-1} is reasonably close to the 18350 cm^{-1} absorption of the gas-phase $\text{Co}(\text{H}_2\text{O})_6^{2+}$ cluster, and the shoulder at 19600 cm^{-1} in the cluster spectrum could be due to absorptions to higher-lying spin-orbit states, or to spin-forbidden transitions³ to doublet states. The intensity of the $4\text{T}_{1\text{g}}(\text{P}) \leftarrow 4\text{T}_{1\text{g}}$ transition is zero by symmetry in an octahedral complex and is calculated to be essentially zero for the relaxed complex. Vibronic coupling to a nonsymmetric vibration could give rise to the observed, weak, intensity. Gilson and Krauss attempted to estimate the extent to which vibronic coupling affects the transition intensity by systematically moving an axial water from its equilibrium position and calculating electronic transition moments.⁵ Distortion from octahedral symmetry by 0.15 \AA only produced an oscillator strength of 10^{-6} . This led them to conclude that $\text{Co}^{2+}(\text{H}_2\text{O})_{6(\text{aq})}$ is not responsible for the aqueous absorption spectrum of $\text{Co}(\text{II})$ solutions. However, based on our observation that $\text{Co}^{2+}(\text{H}_2\text{O})_6$ clusters absorb sufficiently strongly ($\epsilon_{\text{max}} \approx 37\text{ M}^{-1}\text{ cm}^{-1}$) to account for the solution spectrum, and on the similarity between the cluster and solution absorption spectra, on the fact that the hexahydrate is the dominant species in solution,¹ and on the high-temperature studies of cobalt solutions by Swaddle and co-workers,^{9,10} we believe $\text{Co}^{2+}(\text{H}_2\text{O})_{6(\text{aq})}$ is responsible for the observed solution spectrum.

In our earlier study we observed that, from 11900 to 13900 cm^{-1} , $\text{Ni}^{2+}(\text{H}_2\text{O})_6$ dissociates by loss of a single water molecule.¹⁹ In contrast, photodissociation of $\text{Co}^{2+}(\text{H}_2\text{O})_6$ occurs by loss of one or two water molecules, with loss of two waters increasing from 50% of total dissociation at 14900 cm^{-1} to 95% of total dissociation at 21800 cm^{-1} . This trend is exactly what one would expect on the basis of statistical theories of unimolecular dissociation.^{28,29} RRKM calculations show that loss of the first water molecule (to form $\text{Co}^{2+}(\text{H}_2\text{O})_5$) is rapid, but, at lower photon energies, many of the $\text{Co}^{2+}(\text{H}_2\text{O})_5$ ions have insufficient energy to lose a second water molecule during our experimental observation time of $\sim 2\mu\text{s}$. The likelihood of losing the second water molecule increases with photon (and hence, available) energy. The transition between loss of one and two water molecules is not sharp, partly because the $\text{Co}^{2+}(\text{H}_2\text{O})_6$ parent ions are at 300 K and thus have a broad distribution of internal energies. Thus, the different dissociation pathways observed for $\text{Co}^{2+}(\text{H}_2\text{O})_6$ and $\text{Ni}^{2+}(\text{H}_2\text{O})_6$ are at least partially due to the very different photodissociation wavelengths employed in the two studies.

The heptahydrated cluster, $\text{Co}^{2+}(\text{H}_2\text{O})_7$, has a very similar structure to the hexahydrate as it is in effect the hexahydrate chromophore with one water molecule in the outer solvation shell. The spectrum obtained (Figure 1, bottom) is similar to that of the hexahydrate, but is slightly shifted to higher energies (toward the solution spectrum), peaking at 18500 cm^{-1} . At this energy, the estimated cross section is $5 \times 10^{-20}\text{ cm}^2$ ($\epsilon \approx 30\text{ M}^{-1}\text{ cm}^{-1}$). The heptahydrate also shows two dissociation pathways: loss of three waters to form the tetrahydrate or loss of two waters to form the pentahydrate, with the loss of two waters preferred ($>80\%$ over the entire wavelength region examined). Again, this is different from the results for $\text{Ni}^{2+}(\text{H}_2\text{O})_7$, which at lower photon energy dissociates via loss of one or two waters.¹⁹

Pavlov et al.²¹ and Park et al.³⁰ computed the binding energies of $\text{Zn}^{2+}(\text{H}_2\text{O})_n$. Their results show that several nearly isoenergetic structures are possible for each hydrated Zn^{2+} species, for $n \geq 5$. These are described by the number of water molecules

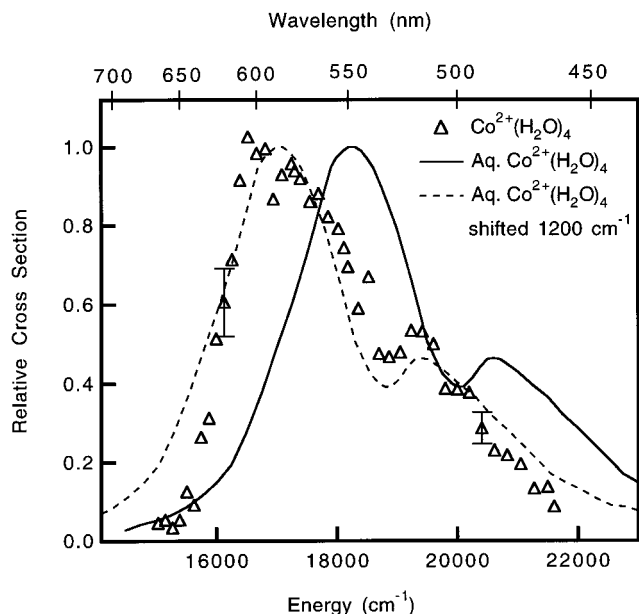


Figure 2. Comparison of total photodissociation spectrum of Co²⁺-(H₂O)₄ (triangles) to the spectrum assigned to aqueous Co²⁺(H₂O)₄ at 497 K by Swaddle and Fabes (ref 9; solid line). Also shown is the aqueous spectrum shifted by 1200 cm⁻¹ to lower energy (dashed line). A relative cross section of one corresponds to $\sigma = 2.5 \times 10^{-19}$ cm² for Co²⁺(H₂O)₄.

in the inner and outer solvation shells and the possible structures for the hexahydrate are 6+0, 5+1 and 4+2. In our earlier study¹⁹ of Ni²⁺(H₂O)_n we found that the tetrahydrate and hexahydrate clusters have very different absorption spectra, with the tetrahydrate spectrum peaking at 570 nm and the hexahydrate peaking near 775 nm. In this study, we find that the absorption maxima of Co²⁺(H₂O)₄ and Co²⁺(H₂O)₆ are much more similar than those of the corresponding nickel clusters, so we have to consider the possibility that the observed dissociation of Co²⁺-(H₂O)₆ could be due to dissociation of a 5+1 or 4+2 isomer. Our data is only consistent with the 6+0 structure being responsible for the observed spectrum. First, the abundance of the pentahydrate and the tetrahydrate clusters in the mass spectrum of Co²⁺(H₂O)_n are both much lower than those of the larger clusters. We would expect much higher abundance for these species if “solvated” small clusters were responsible for the hexahydrate spectrum. Also, if the pentahydrate were formed by adding an outer-shell water to the tetrahydrate (a 4+1 structure), dissociation of the pentahydrate should be observed. This is not the case. Most tellingly, the shape of the photodissociation spectra of the hexa- and heptahydrate clusters is quite different from that of the tetrahydrate. The spectra of the larger clusters are narrower and do not have a pronounced shoulder. In fact, the spectra of the hexa- and heptahydrate clusters are very similar to that of aqueous Co(II), whereas, as discussed below, the spectrum of the tetrahydrate is similar to that of aqueous Co²⁺(H₂O)₄.

Co²⁺(H₂O)₄. Figure 2 shows the total photodissociation spectrum of gas-phase Co²⁺(H₂O)₄. Also shown is the spectrum of aqueous Co²⁺(H₂O)₄ obtained by Swaddle and Fabes from additional bands that appear in the absorption spectrum of aqueous cobalt(II) solutions at high temperature.⁹ The cluster spectrum obtained in this work is red-shifted by 1200 cm⁻¹ from the solution spectrum, with a peak near 17 100 cm⁻¹ and a shoulder at 19 300 cm⁻¹. As the dashed line in Figure 2 shows, once the 1200 cm⁻¹ shift is taken into account, the absorption spectra of the gas phase and aqueous Co²⁺(H₂O)₄ are strikingly

similar. The aqueous spectrum is slightly broader, presumably due to inhomogeneous broadening and a higher temperature (497 K vs 300 K for the gas-phase cluster). The peak photodissociation cross section for Co²⁺(H₂O)₄ is 2.5×10^{-19} cm² ($\epsilon = 150$ M⁻¹ cm⁻¹). The intensity of the tetrahydrate spectrum is a factor of 4 greater than that of the hexahydrate spectrum. The tetrahydrate is expected to absorb significantly more strongly than the hexahydrate because its tetrahedral geometry lacks a center of inversion.^{2,3} As with the hexahydrate, Co²⁺(H₂O)₄ absorbs somewhat more strongly than Ni²⁺(H₂O)₄ which has a peak cross section $\sigma = 7 \times 10^{-20}$ cm².¹⁹ As the tetrahydrate is only a minor species in solution, Swaddle and Fabes were unable to obtain an accurate value for its concentration and hence ϵ . On the basis of analogy with tetrahedral crystals, Swaddle and Fabes propose that the total integrated oscillator strength, f , lies between 2×10^{-3} and 8×10^{-3} for the visible absorption bands of the tetrahydrate.⁹ Our results show that the gas-phase Co²⁺-(H₂O)₄ cluster has $f \approx 2.4 \times 10^{-3}$.

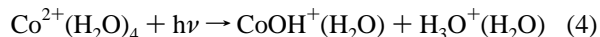
Gilson and Krauss⁵ also suggest that Co²⁺(H₂O)₄ may contribute to the solution spectrum of aqueous Co²⁺ at higher temperatures. They calculate three fairly intense absorption bands at 18 866, 18 900, and 19 707 cm⁻¹, where the splitting is due to a slight distortion from tetrahedral symmetry. As was the case for the hexahydrate, the calculated transition energies for the tetrahydrate are slightly high. Gas-phase Co²⁺(H₂O)₄ has a peak at 17100 cm⁻¹ and a shoulder at 19 300 cm⁻¹. Overall, there is surprisingly good agreement between the positions of the calculated and observed visible absorption bands, especially considering the difficulty of accurately calculating excited electronic states for systems of this complexity. However, the total calculated intensity of the visible absorption bands ($f \approx 2.3 \times 10^{-4}$) is low by a factor of 10, suggesting that, even in the tetrahydrate, the transition derives much of its intensity from vibronic coupling.

Co²⁺(H₂O)₄ Photodissociation Dynamics. The tetrahydrate has two possible dissociation pathways: simple loss of water and charge separation to form two cations



Charge separation is the dominant pathway throughout the energy range studied. Simple loss of water is observed for the tetrahydrate, but is at least an order of magnitude less likely than charge separation. Simple loss of water was not observed for the analogous nickel system.¹⁹ In CID experiments, Kebarle and co-workers observe that dissociation of Co²⁺(H₂O)₄ and Ni²⁺(H₂O)₄ occurs primarily by charge reduction.^{15, 16}

It should be noted that both charged fragments are observed in the difference spectrum. None of the more thermodynamically favorable H₃O⁺(H₂O) which would be formed by



is observed. A small amount of CoOH⁺(H₂O) is observed in the difference spectrum but this is due to secondary photodissociation of the strongly absorbing CoOH⁺(H₂O)₂ species.^{19, 29, 31}

Neglecting the contribution of the photon, a thermochemical cycle for reaction 3 at 298 K can be written as

$$\begin{aligned} \Delta H_{\text{rxn } 3} = & \Delta H_{4,0}(\text{Co}^{2+}) - \text{IP}(\text{Co}^{2+}) + \text{IP}(\text{H}_2\text{O}) + \\ & \text{PA}(\text{OH}) - \text{PA}(\text{H}_2\text{O}) - \text{D}(\text{Co}^+ - \text{OH}) - \\ & \text{D}(\text{CoOH}^+ - \text{H}_2\text{O}) - \text{D}(\text{CoOH}^+ \text{H}_2\text{O} - \text{H}_2\text{O}) \quad (5) \end{aligned}$$

which is an extension of the cycle used by Kebarle.^{15,16} Proton affinities and ionization potentials are taken from standard reference sources.^{32,33} The $\text{Co}^+ - \text{OH}$ bond strength was determined to be 300 ± 4 kJ/mol at 0 K by Armentrout and co-workers³⁴ which corresponds to 298 ± 4 kJ/mol at 298 K, where the thermal correction is based on computed frequencies (see below). The remaining quantities in eq 5 have not been experimentally determined, so computed values are used. The binding energy of four waters to Co^{2+} is estimated as $\Delta H_{4,0^-}(\text{Co}^{2+}) = 1142$ kJ/mol based on theoretical calculations.^{20,21} $D(\text{CoOH}^+ - \text{H}_2\text{O})$ and $D(\text{CoOH}^+\text{H}_2\text{O} - \text{H}_2\text{O})$ were calculated to be 213 and 123 kJ/mol, respectively, using energies and optimized geometries calculated with the B3LYP hybrid density functional and the 6-311++G** basis set for oxygen and hydrogen and the Stuttgart SDD effective core potential for cobalt. Values were converted to 298 K using frequencies calculated at the same level. All calculations were carried out using Gaussian 98.³⁵ Evaluation of the cycle shows the charge separation channel is *exothermic* by 21 kJ/mol in the absence of a photon. As will be discussed in more detail below, the reactants and products are separated by a significant barrier due to the interaction between the attractive $\text{Co}^{2+}(\text{H}_2\text{O})_3 - \text{H}_2\text{O}$ potential and the repulsive $\text{CoOH}^+(\text{H}_2\text{O})_2 - \text{H}_3\text{O}^+$ potential. The presence of this barrier allows for the observation of the thermodynamically unstable $\text{Co}^{2+}(\text{H}_2\text{O})_4$ species.

If reaction 3 proceeded via a direct, inner-shell proton transfer, one would expect most of the available energy to be released as fragment kinetic energy due to the Coulombic repulsion between the like-charged fragments. The kinetic energy release (KER) of this process will lead to a broadening of the fragment ion time-of-flight spectrum. Figure 3 shows an enlargement of the H_3O^+ channel from the difference spectrum obtained at 570 nm with the polarization of the dissociation laser parallel to the ion flight path at low and high reflectron fields. Spectra taken with the polarization perpendicular to the ion path showed no systematic difference. The electric field in the dissociation region of the reflectron maps fragment velocity along the beam axis to relative arrival time at the detector. Kinetic energy release leads to more broadening under low field conditions (108 V/cm) than under the more usual²² high field conditions (205 V/cm). Also shown are simulations^{36,37} for KER of 90, 110, and 130 kJ/mol. The simulations include the spread in parent ion position and velocity and the finite size of the detector (which causes the dip at the center of the peak). The total KER is therefore 110 ± 20 kJ/mol with an anisotropy of $\beta = 0.0 \pm 0.3$. This is consistent with theory which states that photodissociation of a tetrahedral (spherical top) molecule should occur with an anisotropy of zero.³⁸

The resulting KER accounts for about 48% of the available energy in the system. This is similar to the value calculated for nickel, where the KER accounts for 38% of the available energy. For comparison, a direct proton transfer between two inner-shell solvent molecules would result in a much higher KER because the Coulombic repulsion between two singly charged ions is 700 kJ/mol at 2 Å (the typical M–O distance in a hydrated M^{2+}) and only decreases to 110 kJ/mol at 13 Å. The mechanism for photodissociation of $\text{Co}^{2+}(\text{H}_2\text{O})_4$ must account for the modest kinetic energy release and for our observation of dissociation via reaction 3 rather than the more exothermic reaction 4. The similarities between the dissociation pathways and kinetic energy releases we observe¹⁹ for $\text{Ni}^{2+}(\text{H}_2\text{O})_4$ and $\text{Co}^{2+}(\text{H}_2\text{O})_4$ suggest that they dissociate by the same mechanism: a “salt bridge” mechanism. Our proposal of a salt bridge mechanism for charge reduction reactions of transition metal

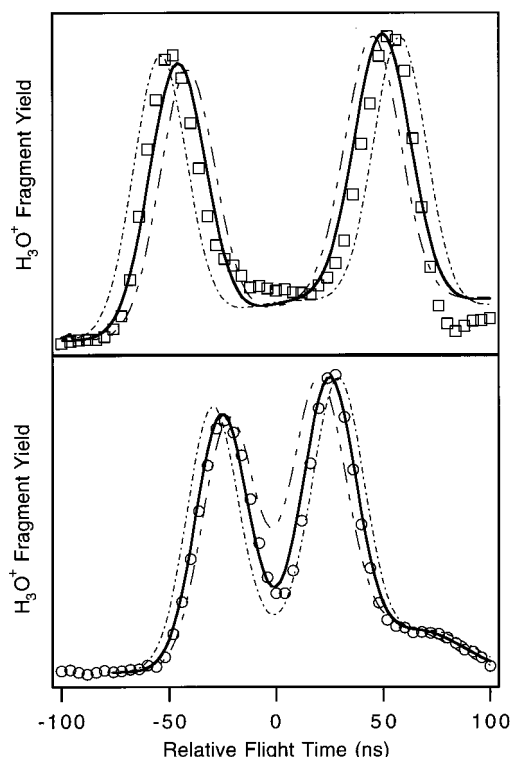
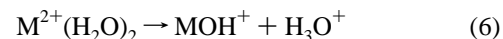


Figure 3. Top, Time-of-flight spectrum of the H_3O^+ fragment produced by photodissociation of $\text{Co}^{2+}(\text{H}_2\text{O})_4$ at 570 nm with the laser polarized parallel to the ion flight path (squares) in a “low” reflectron field. The solid line is a simulation at a total kinetic energy of 110 kJ/mol; simulations at 90 and 130 kJ/mol are shown as dashed lines. Bottom, Time-of-flight spectrum of the H_3O^+ fragment under the same conditions as above, but in a “high” reflectron field (circles). The solid line is a simulation at a total kinetic energy release (KER) of 110 kJ/mol; simulations at 90 and 130 kJ/mol are shown as dashed lines.

dications is based on the work of Beyer et al.³⁹ and Peschke et al.⁴⁰ who carried out density functional calculations of the charge reduction reaction



for the alkaline earth metals. They suggest that the reaction occurs via a mechanism in which a water molecule first moves from the inner solvation shell to the outer shell and then abstracts a proton from a water molecule in the inner solvation shell to form H_3O^+ . At the transition state, the complex forms a salt-bridge configuration $\text{M}^{2+} \cdots \text{OH}^- \cdots \text{H}_3\text{O}^+$. The separation of the positive charges and the Coulombic attraction between the OH^- and H_3O^+ lead to a relatively low KER in the dissociation, with the remainder of the available energy going to internal excitation of the products. Thus, in the salt bridge mechanism for photodissociation of $\text{Ni}^{2+}(\text{H}_2\text{O})_4$ and $\text{Co}^{2+}(\text{H}_2\text{O})_4$, one of the four inner-shell waters first moves to the outer shell, then abstracts a proton and departs. The energetically favorable $\text{H}_3\text{O}^+ \cdots (\text{H}_2\text{O})$ product (reaction 4) is not formed because, at the $(\text{H}_2\text{O})_2\text{M}^{2+} \cdots \text{OH}^- \cdots \text{H}_3\text{O}^+$ transition state, the H_3O^+ is quite far from the remaining water molecules. Detailed calculations by Beyer on the salt bridge mechanism for dissociation of $\text{Co}^{2+}(\text{H}_2\text{O})_4$ are currently underway.⁴¹

Conclusions

The photodissociation spectra of gas-phase $\text{Co}^{2+}(\text{H}_2\text{O})_n$ have been observed for $n = 4, 6,$ and 7 ; the pentahydrate was only present in small amounts and did not dissociate in the energy

range examined in this study. The similarity between the spectrum of gas-phase Co²⁺(H₂O)₆ and the absorption spectrum of aqueous cobalt(II) suggests that Co²⁺(H₂O)_{6(aq)} is responsible for the room-temperature solution absorption spectrum. The observed photodissociation spectrum of Co²⁺(H₂O)₄ is similar to new bands which appear in aqueous cobalt(II) at high temperatures and have been assigned to Co²⁺(H₂O)_{4(aq)} by Swaddle and Fabes.⁹ The hexahydrate dissociates by loss of one or two water molecules, whereas the heptahydrate dissociates by loss of two or three water molecules. In both cases, loss of two water molecules is the preferred dissociation pathway. The tetrahydrate was found to dissociate either by simple loss of water or by charge separation to form CoOH⁺-(H₂O)₂ and H₃O⁺, with charge separation being the preferred dissociation channel. Charge separation produces a kinetic energy release of 110 ± 20 kJ/mol, which represents 48% of the available energy. The "salt bridge" mechanism³⁹ proposed by Beyer et al. predicts the observed products and the modest kinetic energy release.

Acknowledgment. Support for this work by the donors of the Petroleum Research Fund administered by the American Chemical Society is gratefully acknowledged. A Eugene M. Isenberg Award administered by the School of Management at the University of Massachusetts at Amherst for partial funding of Kieron Faherty is also gratefully acknowledged.

References and Notes

- Ohtaki, H.; Radnai, T. *Chem. Rev.* **1993**, *93*, 1157–1204.
- Sutton, D. *Electronic Spectra of Transition Metal Complexes*; McGraw-Hill: London, 1968.
- Lever, A. B. P. *Studies on Physical and Theoretical Chemistry: Inorganic Electronic Spectroscopy (Second Edition)*; Elsevier: Amsterdam, 1984.
- Cotton, F. A.; Wilkinson, G. W. *Advanced Inorganic Chemistry*; Wiley: London, 1988.
- Gilson, H. S. R.; Krauss, M. *J. Phys. Chem. A* **1998**, *102*, 6525–6532.
- Rotzinger, F. P. *J. Am. Chem. Soc.* **1996**, *118*, 6760–6766.
- Rotzinger, F. P. *J. Am. Chem. Soc.* **1997**, *119*, 5230–5238.
- Tsutsui, Y.; Wasada, H.; Funahashi, S. *Bull. Chem. Soc. Jpn.* **1998**, *71*, 1771–1779.
- Swaddle, T. W.; Fabes, L. *Can. J. Chem.* **1980**, *58*, 1418–1426.
- Fedorchuk, C.; Swaddle, T. W. *J. Phys. Chem. A* **2000**, *104*, 5651–5652.
- Gilson, H. S. R.; Krauss, M. *J. Phys. Chem. A* **2000**, *104*, 5653–5654.
- Freiser, B. S. *Understanding Chemical Reactivity: Organometallic Ion Chemistry*; Kluwer Academic Publishers: Dordrecht, 1996.
- Keese, R. G.; A. W. Castleman, J. *J. Phys. Chem. Ref. Data* **1986**, *15*, 1011–1071.
- Yamashita, M.; Fenn, J. B. *J. Phys. Chem.* **1984**, *88*, 4451–4459.
- Blades, A. T.; Jayaweera, P.; Ikonomou, M. G.; Kebarle, P. *Int. J. Mass Spec. Ion Proc.* **1990**, *102*, 251–267.
- Blades, A. T.; Jayaweera, P.; Ikonomou, M. G.; Kebarle, P. *J. Chem. Phys.* **1990**, *92*, 5900–5906.
- Spence, T. G.; Burns, T. D.; Guckenberger, G. B.; Posey, L. A. *J. Phys. Chem. A* **1997**, *101*, 1081–1092.
- Spence, T. G.; Trotter, B. T.; Posey, L. A. *J. Phys. Chem. A* **1998**, *102*, 7779–7786.
- Thompson, C. J.; Husband, J.; Aguirre, F.; Metz, R. B. *J. Phys. Chem. A* **2000**, *104*, 8155–8159.
- Åkesson, R.; Pettersson, L. G. M.; Sandström, M.; Siegbahn, P. E. M.; Wahlgren, U. *J. Phys. Chem.* **1992**, *96*, 10 773–10 779.
- Pavlov, M.; Siegbahn, P. E. M.; Sandström, M. *J. Phys. Chem. A* **1998**, *102*, 219–228.
- Husband, J.; Aguirre, F.; Ferguson, P.; Metz, R. B. *J. Chem. Phys.* **1999**, *111*, 1433–1437.
- Chien, B. M.; Michael, S. M.; Lubman, D. M. *Int. J. Mass Spectrom.* **1994**, *131*, 149–179.
- Michael, S. M.; Chien, B. M.; Lubman, D. *Anal. Chem.* **1993**, *65*, 2614–2620.
- Posey, L. A.; DeLuca, M. J.; Johnson, M. A. *Chem. Phys. Lett.* **1986**, *131*, 170–174.
- Rodriguez-Cruz, W. E.; Jockusch, R. A.; Williams, E. R. *J. Am. Chem. Soc.* **1998**, *120*, 5842–5843.
- Rulíšek, L.; Havlas, Z. *J. Chem. Phys.* **2000**, *112*, 149–157.
- Rodgers, M. T.; Ervin, K. M.; Armentrout, P. B. *J. Chem. Phys.* **1997**, *106*, 4499–4508.
- Thompson, C. J.; Aguirre, F.; Husband, J.; Metz, R. B. *J. Phys. Chem. A* **2000**, *104*, 9901–9905.
- Lee, S.; Kim, J.; Park, J. K.; Kim, K. S. *J. Phys. Chem.* **1996**, *100*, 14 329–14 338.
- Cassady, C. J.; Freiser, B. S. *J. Am. Chem. Soc.* **1984**, *106*, 6176–6179.
- Hunter, E. P.; Lias, S. G. Proton Affinity Evaluation In *NIST Chemistry WebBook, NIST Standard Reference Database Number 69*; Mallard, W. G., Linstrom, P. J., Eds.; National Institute of Standards and Technology: Gaithersburg, MD, February 2000. (<http://webbook.nist.gov>).
- Weast, R. C. *Handbook of Chemistry and Physics*; CRC Press: Boca Raton, FL, 1985.
- Armentrout, P. B.; Kickel, B. L. in *Organometallic Ion Chemistry*; Freiser, B. S., Ed.; Kluwer Academic Publisher: Dordrecht, 1996; pp 1–45.
- Frisch, M. J.; Trucks, G. W.; Schlegel, H. B.; Scuseria, G. E.; Robb, M. A.; Cheeseman, J. R.; Zakrzewski, V. G.; Montgomery, J. A.; Stratmann, R. E.; Burant, J. C.; Dapprich, S.; Millam, J. M.; Daniels, A. D.; Kudin, K. N.; Strain, M. C.; Farkas, O.; Tomasi, J.; Barone, V.; Cossi, M.; Cammi, R.; Mennucci, B.; Pomelli, C.; Adamo, C.; Clifford, S.; Ochterski, J.; Petersson, G. A.; Ayala, P. Y.; Cui, Q.; Morokuma, K.; Malick, D. K.; Rabuck, A. D.; Raghavachari, K.; Foresman, J. B.; Cioslowski, J.; Ortiz, J. V.; Stefanov, B. B.; Liu, G.; Liashenko, A.; Piskorz, P.; Komaromi, I.; Gomperts, R.; Martin, R. L.; Fox, D. J.; Keith, T.; Al-Laham, M. A.; Peng, C. Y.; Nanayakkara, A.; Gonzalez, C.; Challacombe, M.; Gill, P. M. W.; Johnson, B. G.; Chen, W.; Wong, M. W.; Andres, J. L.; Head-Gordon, M.; Replogle, E. S.; Pople, J. A. *Gaussian 98 Revision A.3* (Gaussian, Inc., Pittsburgh, PA, 1998).
- Ding, L. N.; Kleiber, P. D.; Young, M. A.; Stwalley, W. C.; Lyyra, A. M. *Phys. Rev. A* **1993**, *48*, 2024–2030.
- Cheng, Y. C.; Chen, J.; Klieber, P. D.; Young, M. A. *J. Chem. Phys.* **1997**, *107*, 3758–3765.
- Yang, S.-C.; Bersohn, R. *J. Chem. Phys.* **1974**, *61*, 4400–4407.
- Beyer, M.; Williams, E. R.; Bondybey, V. E. *J. Am. Chem. Soc.* **1999**, *121*, 1565–1573.
- Peschke, M.; Blades, A. T.; Kebarle, P. *Int. J. Mass Spectrom.* **1999**, *185*, 685–699.
- Beyer, M., personal communication.